

The Influence Of Elastic Deformations On The Supersolid Transition

T. Arpornthip,^{1,2} A. V. Balatsky,^{2,3} M. J. Graf,² and Z. Nussinov¹

¹ *Department of Physics, Washington University, MO 63160 USA*

² *Theoretical Division, Los Alamos National Laboratory, Los Alamos, New Mexico 87545 USA*

³ *Center for Integrated Nanotechnologies, Los Alamos National Laboratory, New Mexico 87545 USA*

(Dated: July 23, 2022)

We highlight how an elastic deformation in a supersolid leads to local change in supersolid transition temperature. Different types of elastic deformations are studied. We find that contraction/compression of the medium leads to higher /lower transition temperatures. The local change in transition temperature, if the effect is observable, could lead to interesting phenomena. For example, in the case of contraction edge displacement, the edges of the crystal could decouple from the bulk solid if the whole sample is put in a torsional oscillator. This effect may lead to a change in the torsional oscillator period.

PACS numbers:

I. INTRODUCTION

Superfluids flow without any resistance. The existence of superfluidity raises the possibility of supersolids^{1,2}-solids in which superfluidity can occur without disrupting crystalline order. Long ago, Chester² theoretically demonstrated the possible existence of a supersolid. If supersolid could exist, a natural contender would be solid Helium.³ Recent torsional oscillator experiments⁴ on solid ⁴He pointed to supersolid type features and have led a flurry of activity.⁶ In the simplest explanation of the experiments,⁴ a portion of the medium becomes, at low temperatures, a superfluid that decouples from the measurement apparatus. Such a “Non Classical Rotational Inertia” (NCRI) effect is known to exist in superfluid liquid Helium^{7,8} which was probed with similar techniques.^{8,9} Experimental results suggest the absence of superfluid features in ideal crystals with no grain boundaries.⁵ Currently, it is not clear if an NCRI lies at the core of the recent experimental findings in solid ⁴He. For instance, the required condensate fraction adduced from a simple NCRI-only explanation does not simply conform with thermodynamic measurement¹⁰. Rittner and Reppy¹¹ discovered that the putative super-solid type feature is acutely sensitive to the quench rate for solidifying the liquid. Aoki, Keiderling, and Kojima reported rich hysteresis and memory effects¹². Such effects can arise from glassy characteristics alone^{10,13}. The presence of non-uniformity in ⁴He is also suggested by a criterion comparing the change in dissipation vs. relative period shift in torsion oscillator.¹⁴ It may well be that these glassy and superfluid effects are present in solid Helium.¹⁵ An interesting question concerns the coupling between elastic defects such as dislocations and superfluid type features.¹⁶ The coupling of the supersolid transition to impurities was discussed in Ref. 17. The coupling between superfluidity and elasticity in supersolids and how this may lead to a strain-dependent critical temperature was discussed in Refs. 18,19. The viable existence of supersolid phase is not confined to solid Helium. A supersolid state of cold atoms in a confining optical lattice

was very recently achieved²¹. There has been much work examining supersolidity in spin systems as well, see for e.g., Ref. 22. Supersolids constitute a fascinating state of matter and appear in a host of systems.

This article focuses on the coupling between nanoscale structure and supersolidity^{18,19,20}. As is well appreciated, elastic strain may fundamentally affect local and mesoscopic electronic, magnetic and structural properties. There is ample evidence for significant coupling amongst the electronic degrees of freedom with the lattice distortions in cuprates, manganites, and ferroelectrics.^{23,24} The central thesis of this work is that *elastic distortions may lead to a sizable measurable effect of the supersolid behavior*. As we will elaborate later on, in, e.g., a cylindrical torsional oscillator geometry in which the boundary of the solid is elastically deformed so that it undergoes a supersolid transition at a lower temperature than the bulk, a decoupling of the bulk from the torsional oscillator chassis will occur and lead to a measurable reduction in the period.

In this work, we will employ a Ginzburg-Landau (GL) theory to study the influence of elastic strain on supersolidity. As we will show, the Euler-Lagrange equations for the GL free energy result in an effective Schrödinger type equation. We find the lattice distortion acts as an effective potential for the supersolid order parameter. Solving the resulting effective Schrödinger type equation, we find our main result: A contraction of the lattice edges and its expansion lead to an elevation/decrease in the local supersolid transition temperature.

The outline of the paper is as follows: in Section(II), we set up the general GL framework for our investigations. We illustrate the connection between the Euler-Lagrange equation and the Schrödinger equation. In the sections thereafter, we focus on particular lattice distortion profiles to determine the change in the local supersolid transition temperature. In Section(III), we examine the influence of a boundary edge contraction, and in section(IV), we study the opposite case of a boundary edge expansion.

II. GENERAL FRAMEWORK

We study the GL free energy density

$$F = a(T)|\psi|^2 + \frac{1}{2}b|\psi|^4 + c|\nabla\psi|^2 + \lambda(\vec{r})|\psi|^2, \quad (1)$$

where T is the temperature, b and c being positive constants, ψ the (complex) supersolid order parameter, and $\lambda(\vec{r})$ a position dependent coupling that captures the coupling of the order parameter to elastic strain as we elaborate on below. The prefactor b in Eq.(1) is positive and depends only on the density of the crystal²⁵. For temperatures $T < T_c$, the coefficient $a(T)$ is negative enabling a non-zero ψ to minimize the free energy.²⁶ The condition $a(T_c) = 0$ determines the transition temperature $T = T_c$ below which supersolidity onsets.²⁵ The third term in Eq.(1) relates the free energy with the magnitude of the gradient of ψ , as in a domain wall²⁶. The difference between the free energy of a normal crystal and a displaced crystal appears in the last term. For a crystal whose constituents i undergo a distortion from an ideal unperturbed configuration \vec{R} to a shifted configuration \vec{R}' due to the application of stresses, we set $\vec{u}_i = \vec{R}'_i - \vec{R}_i$ and take the continuum limit wherein we replace i by the continuous coordinate \vec{r} . In the up and coming, the Greek indices α, β will denote the spatial components (e.g., $u_{\alpha=1,2,3}$ will denote the Cartesian components of the displacement \vec{u} at site \vec{r}). In general, a linear coupling of the form $a_{\alpha\beta}u_{\alpha\beta}|\psi|^2$ is allowed between the linear order strain tensor $u_{\alpha\beta} = \frac{1}{2}(\partial_\alpha u_\beta + \partial_\beta u_\alpha)$ (where \vec{u} is the elastic displacement)²⁷ and the supersolid order parameter ψ .^{18,28} In what follows, we will consider, for simplicity, the case in which the displacement occurs only along one Cartesian direction. Allowing for general displacements does not change our conclusions. For uni-directional displacements, the coefficient of the last term in Eq.(1) can be expressed as

$$\lambda(\vec{r}) = d\vec{\nabla} \cdot \vec{u}(\vec{r}), \quad (2)$$

where d is a positive constant and $u(r)$ is the uni-directional displacement field. The sign of d is chosen such that the free energy of Eq.(1) is lowered on introducing vacancies (the vacancy density scales with $[-(\vec{\nabla} \cdot \vec{u})]$). Eq.(2) and the free energy are functions of the strain tensor and thus symmetric under spatial reflections under which $\vec{r} \rightarrow -\vec{r}$ and $\vec{u} \rightarrow -\vec{u}$. In bulk linear elasticity, the local strains scale, as in Hooke's law, as the pressure divided by the elastic moduli. In the following sections, we will consider the strain fields associated with various cases. This last term in Eq.(1) results from a coupling between the displacement and the order parameter. In the cases that we will examine the displacement \vec{u} will occur along one Cartesian direction (\vec{u} will have only one component). Furthermore, in the first two cases that we will detail below (contraction and expansion along an edge), this displacement field will vary only along one Cartesian direction and will be uniform along all other orthogonal

directions. Consequently, the coupling λ will depend only on one Cartesian direction: $\lambda = \lambda(z)$. In the last case discussed in this work, that of an edge dislocation, the displacement field (and consequently the coupling λ) will depend on two directions.

To find the ground state of such crystal, we want to minimize the free energy. The variational derivative of F with respect to ψ^* leads to the Euler-Lagrange equation

$$\frac{\delta F}{\delta \psi^*} = a(T)\psi + b|\psi|^2\psi - c\nabla^2\psi + \lambda(\vec{r})\psi = 0, \quad (3)$$

with an identical (complex conjugated) equation for $\delta F/\delta\psi = 0$. In situations in which a weakly first- or second-order supersolid transition occurs, we may omit the cubic term in Eq.(3),²⁹ and the variational equation may be recast as

$$-c\nabla^2\psi + \lambda(\vec{r})\psi = -a(T)\psi. \quad (4)$$

Eq.(4) is a Schrödinger type equation with $c = \hbar^2/2m$ and $a(T) = -E$ with E the energy and m a mass. Solving for the eigenvalue $E = -a(T)$ enables us to extract the transition temperature. Generally, a shift in the transition temperature results from the coupling to the elastic displacements.

The gradients of \vec{u} as embodied in $\lambda(\vec{r})$, take on the role of a potential energy in the effective quantum problem for the “wavefunction” ψ .

In the remainder of this work, we will examine the solutions of Eq.(4) for various elastic strains u . In particular, we will examine the strain fields associated with a contraction of the sample boundaries, an expansion of a boundary edge, and the strain profile associated with an edge dislocation.

III. CONTRACTION OF BOUNDARY EDGE

Consider a crystal with a side of length L (the coordinate values corresponding to this side are in the range $L/2 \geq z \geq -L/2$). Near the two edges, the lattice sites are most displaced from their equilibrium positions, see Fig.(??). This displacement at the edges causes a local change in transition temperature.

The nature of the contraction is described by the displacement function u . A contraction can be written in terms of two Gaussian, one for the left end ($z = -L/2$) and the other for the right end,

$$u = \begin{cases} u_0[e^{-(z+L/2)^2/k^2} - e^{-(z-L/2)^2/k^2}] & \text{for } |z| \leq L/2 \\ 0 & \text{for } |z| > L/2 \end{cases}, \quad (5)$$

with k an arbitrary constant and u_0 the maximum displacement. As there are no sites of which $|z| > L/2$, $u = 0$ in that range. With a suitable choice of k in relative to L , we can limit the lattice sites displaced by u to the edge regions only, while leaving the majority of the lattice sites unaltered. For contracting edges, the slope

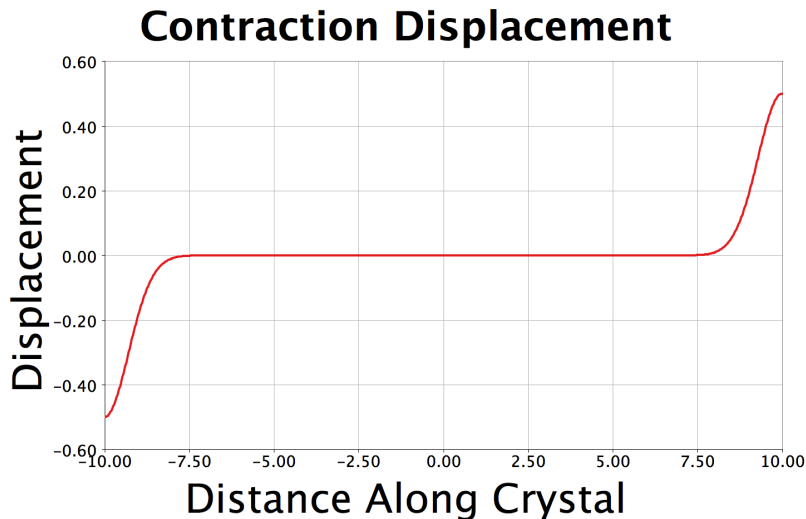


Figure 1: The displacement field corresponding to a contraction near the edges. In this sketch, the displacement is given by Eq.(5) with $L = 20$, $u_o = 0.5$, and $k = 1$ where the lattice constant set to unity.

of u is always negative. Therefore, the energy E in the Schrödinger like equation of Eq.(4) which we wish to minimize may attain negative values. The effective potential is given by

$$\lambda = \frac{2u_0d}{k^2} \left[\left(z - \frac{L}{2} \right) e^{-(z-\frac{L}{2})^2/k^2} - \left(z + \frac{L}{2} \right) e^{-(z+\frac{L}{2})^2/k^2} \right]. \quad (6)$$

For small deformations, this attractive potential leads to the appearance of a weak bound state. For $z > 0$, $L/2 \gg (L/2 - z) \gg k\sqrt{\ln(2u_0d/k)} \equiv \epsilon/2$, the effective potential tends to zero, and the bound state wavefunction is of the form $\psi \sim \exp[\kappa(z - L/2)]$. A similar form is attained near the point $z = -L/2$. The value of κ and thus of the bound state energy $E = -c\kappa^2$ can be computed in the standard way by integrating the Schrödinger equation once in a region of width ϵ across the point $z = L/2$ in an extension of the problem to $z > L/2$ in which the potential is symmetrized about the point $z = L/2$. As $|E| \ll |\lambda(z)|$ in the narrow region near the edges, Eq.(4) reads

$$-2\kappa = \left[\frac{d\psi}{dz} \right]_{L/2-\epsilon/2}^{L/2+\epsilon/2} = \frac{1}{c} \int_{L/2-\epsilon}^{L/2+\epsilon} \lambda(z) dz. \quad (7)$$

Ignoring exponentially small corrections, we attain that the bound state energy is

$$E = -\frac{d^2u_0^2}{4c}. \quad (8)$$

We will now employ the value of E to determine a change in the transition temperature. From the GL theory, $a(T) \simeq \alpha(T - T_c^o)$ near the transition temperature, where T_c^o is the unaltered transition temperature and $\alpha > 0$ is a constant. Writing $a + E = \alpha(T - T_c^{eff})$ where T_c^{eff} is the effective transition temperature, we have

$$T_c^{eff} = T_c^o + \frac{d^2u_0^2}{4\alpha c}. \quad (9)$$

In other words, the region near the edges has a *higher transition temperature into the supersolid state*. The effect of this shifted transition temperature is that, when a sample of contracted ^4He is cooled down, the region near the edges would turn into supersolid at a higher temperature than the bulk of the crystal. Returning to the NCRI^{4,7,8,9} briefly discussed in the introduction, if the entire sample is rotating before the transition to a supersolid phase occurs, at some temperature higher than the normal transition to supersolid of bulk helium but low enough to make the edges become supersolid, the edges will decouple from the bulk rotation and remain stationary, while the bulk crystal keeps rotating. This situation is depicted schematically in Figures (2, 3). This is, essentially, a manifestation of a supersolid transition occurring at the two faces of the crystal before the transition of the bulk crystal which appears at lower temperatures. If this occurs in such an experiment, then the interior within the bulk might decouple partially from the external rotating chassis attached at the edge even though it has not undergone a supersolid transition. This may occur if the edge becomes partially decoupled from the external chassis leading to a reduced coupling between the bulk to the external rotating drive.

As the displacement only occurs near the edges, and since the change in transition temperature is the result of the displacement, it is reasonable to assume that the change in transition temperature can only be detected in the region near the edges. For the region inside the crystal (far from the edge), the transition temperature should remain unaltered. Based on the observation, the transition temperature as a function of the z -axis (the axis parallel to the length of the crystal) could be described as

$$T_c^{eff}(z) = T_c^o + f(z) \left(\frac{d^2u_0^2}{4\alpha c} \right), \quad (10)$$

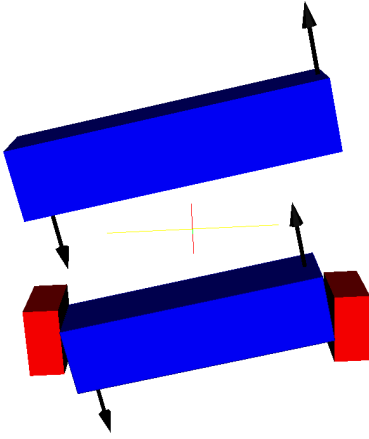


Figure 2: The top crystal shows the rotation before the transition to supersolid of the edges occurs. The bottom crystal depicts the situation when the edges have turned supersolid and decoupled from the bulk, while the bulk crystal still remains a normal solid.

where $f(z)$ is a function that rapidly varies from 1 at the boundaries $z = \pm L/2$ to zero for positions removed from the boundaries. An example is provided by

$$f(z) = e^{-(z-L/2)^2/k^2} + e^{-(z+L/2)^2/k^2}. \quad (11)$$

A contour plot of T_c^{eff} is depicted in figure 4, for $L = 20$, $k = 1$, $T_c^o = 2$, $u_o = 0.5$ and $\frac{d^2}{4\alpha c} = 0.2$.

IV. EXPANSION OF EDGE BOUNDARIES

The situation of the expansion of near the edge boundaries is schematically shown in Figure ???. A typical displacement field u is, in this case, given by

$$u = \begin{cases} u_o [e^{-(z-L/2)^2/k^2} - e^{-(z+L/2)^2/k^2}] & \text{for } |z| \leq L/2 \\ 0 & \text{for } |z| > L/2 \end{cases}. \quad (12)$$

As in our earlier study, the variational equations give rise to a Schrödinger equation. However, as the sign of u is changed, the sign of λ is flipped. In this case, λ is everywhere positive reflecting a repulsive effective potential. This difference in sign gives rise to an important difference between expansion and contraction. In the case of expansion, the effective potential displays two peaks instead of two wells. In the absence of the two peaks, the problem reduces to that of a particle in an infinite potential well model. The wavefunction for the unperturbed ground state is given by

$$\psi = \sqrt{\frac{2}{L}} \cos\left(\frac{\pi}{L}z\right). \quad (13)$$

The energy of such state is

$$E = \frac{\pi^2 c}{L^2}. \quad (14)$$

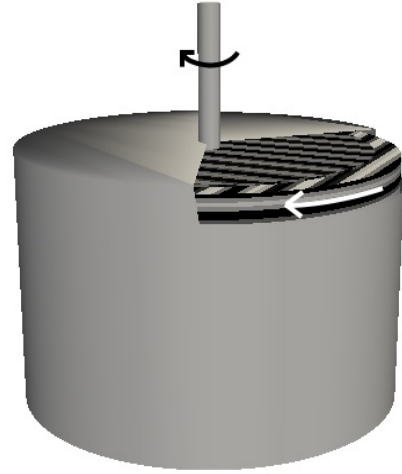


Figure 3: Side view of the effect illustrated in Fig.(2) highlighting the decoupling of the rim motion from the chassis (see different arrows). Under compression of the edges of the torsional oscillator, the rim becomes a supersolid at a higher temperature than the bulk does. On cooling down to this temperature, the rim decouples from the outer chassis and moves at a different angular speed. Consequently, the bulk- although not a supersolid- also decouples from the outer chassis. This results in a pronounced torsional oscillator effect wherein the outer chassis has a lower period than it does at temperatures above the supersolid transition temperature of the outer rim.

Now, consider the perturbed state with the potential given by $\lambda = \vec{d} \cdot \vec{\nabla} u$. We may replace the two Gaussians by two delta functions at the two maximum values of λ . These two values can be easily found by taking the derivative of λ with respect to z and set it equal to zero. The two values are $z = \mp \frac{L}{2} \pm \frac{k}{\sqrt{2}}$. We can write λ as

$$\lambda = du_o \left[\delta\left(z - \left(\frac{L}{2} - \frac{k}{\sqrt{2}}\right)\right) + \delta\left(z + \left(\frac{L}{2} - \frac{k}{\sqrt{2}}\right)\right) \right]. \quad (15)$$

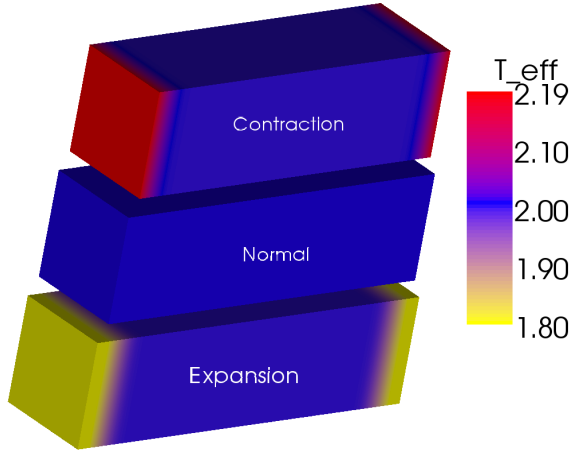
The first order approximation of the perturbed ground state energy is

$$E' = E + \int_{-\infty}^{\infty} \psi^* \lambda \psi dz = E + \frac{8du_o}{\pi} \sin \frac{k\pi}{L\sqrt{2}}. \quad (16)$$

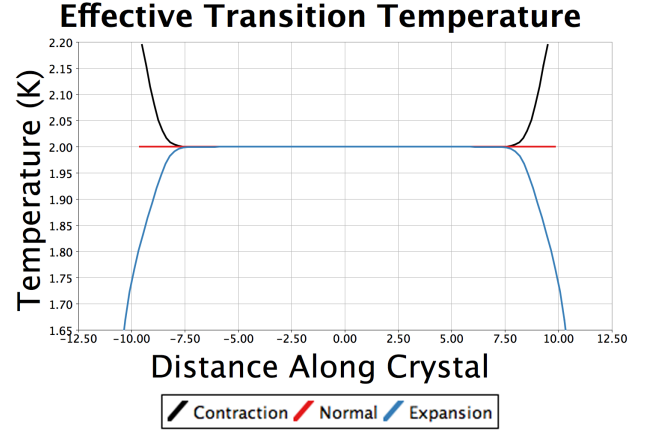
Replicating the same steps as in the previous section, we find that the effective transition temperature T_c^{eff} for the case of expansion is

$$T_c^{eff}(z) = T_c^o - f(z) \cdot \left(\frac{\pi^2 c}{\alpha L^2} + \frac{8du_o}{\alpha\pi} \sin \frac{k\pi}{L\sqrt{2}} \right).$$

In this case, as the system is cooled down, the faces would become supersolid after the bulk crystal as we cool down the crystal. A plot is given as Figure 4 for $T_c^o = 2$, $u_o = 0.5$, $\frac{\pi^2 c}{\alpha L^2} = 0.02$, and $\frac{8d}{\alpha\pi} \sin \frac{k\pi}{L\sqrt{2}} = 1$.



(a) Spatially dependent supersolid transition temperature of slab



(b) Spatial profile of supersolid transition temperature along slab

Figure 4: The transition temperature along a slab is plotted in a contour map for different cases from top to bottom: a slab with contraction, a uniform slab, and a slab with expansion near its edges. Whenever the elastic deformations are present, the local supersolid transition temperature is altered by comparison to the uniform solid. Near the edges, where the elastic deformation is present, the supersolid transition temperature is altered: T_c increases at the boundaries in the case of boundary contraction and decreases for an expansion near the boundaries. The dark (black) line is associated with contraction, red line with the normal crystal, and blue with the expansion. Color online.

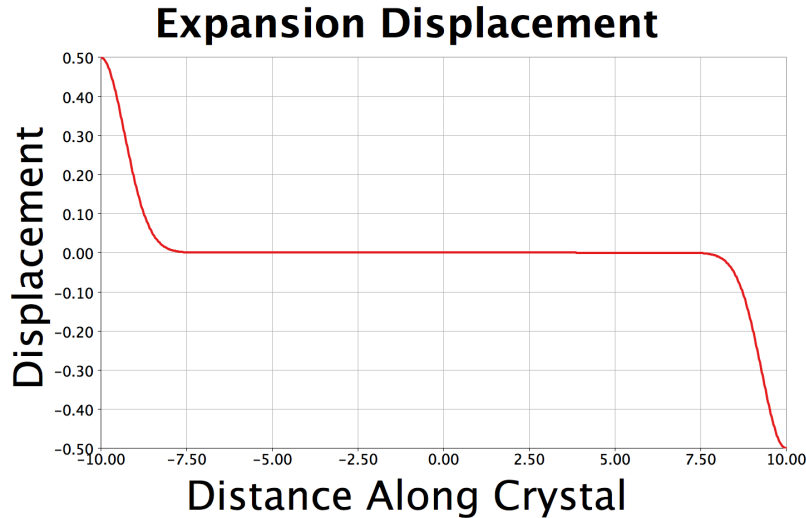


Figure 5: The displacement field corresponding to an expansion near the edges. Plotted is the displacement field given by Eq.(12) with $L = 20$, $u_0 = 0.5$, and $k = 1$.

It is worth highlighting the origin of the difference between the cases of edge contraction and expansion. Both cases have different divergences of the displacement field (and thus different local density profiles). The local mass (or equivalently, the vacancy) density is what couples to the supersolid order parameter. Both the displacement field and the spatial gradient are odd under spatial reflection. In our case, the divergence of u is even under spatial reflection (it reflects the scalar mass density) and the two cases are physically very different even though

the spatial profile of the displacement fields in both cases are related by a minus sign (see Eqs.(5, 12)).

V. CONCLUSIONS

In summary, we find that elastic deformation in supersolid leads to local changes in transition temperature. For a positive coupling constant d in Eq.(2), an

1. Edge contraction increases the supersolid transition

temperature at and near the edges.

2. Edge expansion decreases the supersolid transition temperature at and near the edges.

This implies the observation of interesting effects. For example, for edge contraction, we would find that, below a certain temperature that is higher than the supersolid transition temperature, a sample of supersolid would have its edges decoupling from its bulk crystal. In a cylindrical torsional oscillator realization,⁴ this decoupling would imply that the bulk He would no longer move with the chassis and, see Figs.(2, 3), and thus *the effective moment of inertia of the system would be dramatically lowered*. This would lead to a huge effect in the torsional oscillator measurements. This prediction can be experimentally measured. The above conclusions were based on the assumption of a positive coupling constant d in Eq.(2). Formally, for negative d , our conclusions would have been inverted- an expansion would elevate the local supersolid transition while a contraction would reduce the supersolid transition temperature.

Similar effects are found elsewhere in regions that locally expand or contract. In the appendix, we discuss the case of an edge dislocation. Following the same analysis as before, we show that near an edge dislocation the local supersolid transition temperature may be elevated relative to its value in the bulk.¹⁹

VI. ACKNOWLEDGMENTS

This work was partially supported by the Center for Materials Innovation (CMI) of Washington University, St. Louis and by the US Dept. of Energy at Los Alamos National Laboratory under contract No. DE-AC52-06NA25396. We are grateful to A. T. Dorsey, J. Beamish, and J. C. Davis for many stimulating discussions.

VII. DISLOCATION

Below, we will present a calculation for an edge dislocation. A similar analysis may be done for a screw dislocation.²⁷ For a discussion of dislocations in the quantum arena see¹⁶. A schematic diagram of an edge dislocation is presented in Figure 6(a). A Cartesian coordinate form for a displacement field associated with an edge dislocation is

$$\vec{u}(x, y) = -\frac{b}{2\pi} e^{-(x^2+y^2)/k^2} \text{sgn}(x) \cos^{-1} \left(\frac{-y}{\sqrt{x^2+y^2}} \right) \hat{x}, \quad (17)$$

where $\text{sgn}(x)$ is the sign of x , i.e., $\text{sgn}(x) = [2\theta(x) - 1]$ with $\theta(x)$ the Heavyside function. The vector field of the dislocation is depicted in Fig. 6(b).

We derive an effective potential from the displacement in the same way we did for the above two cases (Eq.(2)).

In this case, an analytical solution to Schrödinger equation is not possible and we will resort to a numerical solution. The effective potential energy is provided in Figure 7.

We approximate the partial derivatives in Schrödinger equation by finite differences and use the Gauss-Seidel method for solving iteratively a system of linear equations in conjunction with overrelaxation. Our relaxation scheme shows that the wavefunction localizes rapidly to the region near the origin. Both the initial seed and the final numerical result are depicted in figure 8. The solution to the Schrödinger equation illustrates that there is a change in transition temperature. A contending variational state that is localized about the origin is given by

$$\psi(x, y) = \sqrt{\frac{2\sigma}{\pi}} e^{-\sigma(x^2+y^2)}. \quad (18)$$

From Eq. (17), we can compute the effective potential energy,

$$\begin{aligned} V &\equiv \lambda = d(\vec{\nabla} \cdot \vec{u}) \\ &= \frac{bd}{2\pi} \text{sgn}(x) e^{-\sigma(x^2+y^2)} \left[\frac{2x}{k^2} \cos^{-1} \left(\frac{-y}{\sqrt{x^2+y^2}} \right) \right. \\ &\quad \left. + \frac{y}{x(x^2+y^2)} \right]. \end{aligned} \quad (19)$$

The Hamiltonian $H = [-c\nabla^2 + V]$ corresponds to the Schrödinger equation of Eq. (4). The expectation value

$$\langle H \rangle = 2c\sigma - \frac{\sigma bd}{2\sqrt{\pi k^2(2\sigma + \frac{1}{k^2})^3}} \geq E_{ground}. \quad (20)$$

An extremizing variational value of σ is given by

$$\sigma = \frac{1}{2} \left(\left(\frac{3bd}{8\sqrt{\pi}ck^4} \right)^{2/5} - \frac{1}{k^2} \right). \quad (21)$$

Substituting the above equation into Eq.(20), we obtain

$$\langle H \rangle = c\left(\beta - \frac{1}{k^2}\right) - bd \left(\frac{\beta k^2 - 1}{4\sqrt{\pi}\beta^3 k^4} \right), \quad (22)$$

where $\beta = \left(\frac{3bd}{8\sqrt{\pi}ck^4} \right)^{2/5}$. Similar to the earlier two cases of boundary deformations, the effective transition temperature can be found by approximating $a(T) \approx \alpha(T - T_c^0)$. The transition temperature

$$T_c^{eff} = T_c^0 - \frac{1}{\alpha} c \left(\left(\beta - \frac{1}{k^2} \right) + bd \left(\frac{\beta k^2 - 1}{4\sqrt{\pi}\beta^3 k^4} \right) \right). \quad (23)$$

For $k < 8\sqrt{\pi}c/(3bd)$, the local supersolid transition temperature is elevated by comparison to that of the undeformed solid.

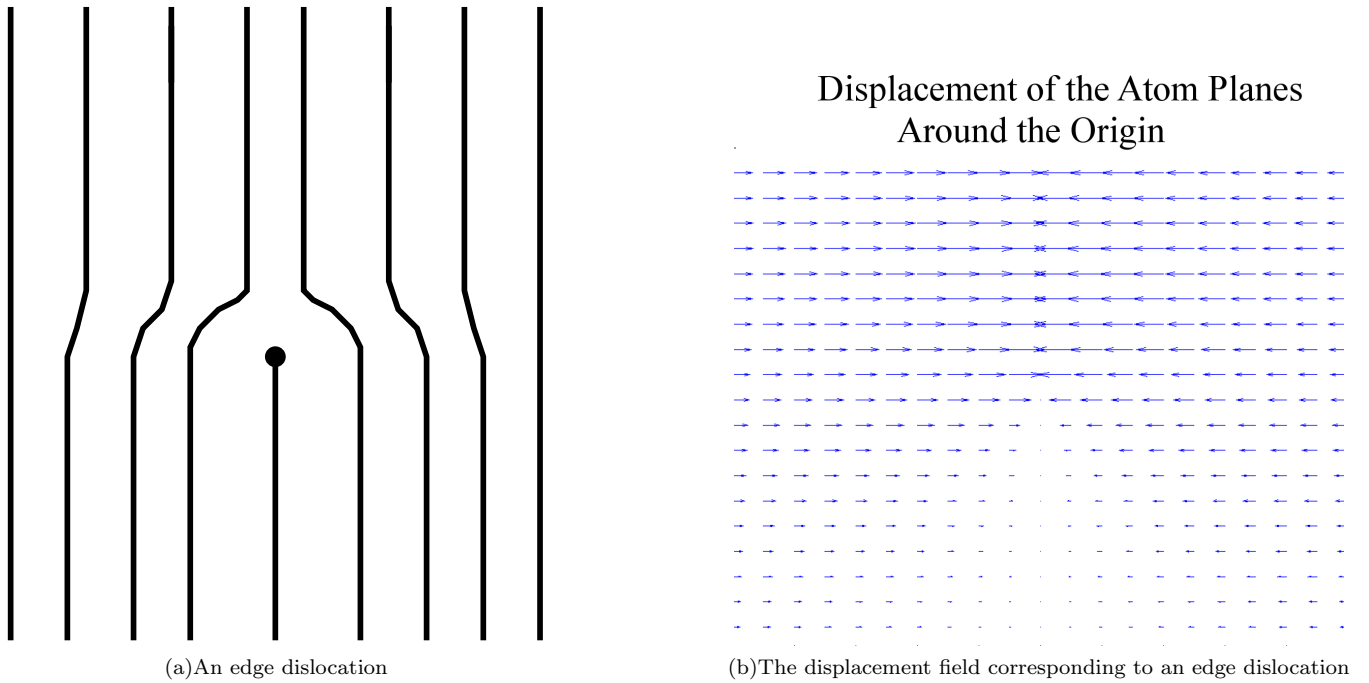


Figure 6: A schematic of an edge dislocation. At left, shown are rows of atoms. The presence of an edge dislocation is manifest in the appearance of a different number of vertical rows of atoms above and below the terminal dislocation point. The corresponding displacement field is shown at right.

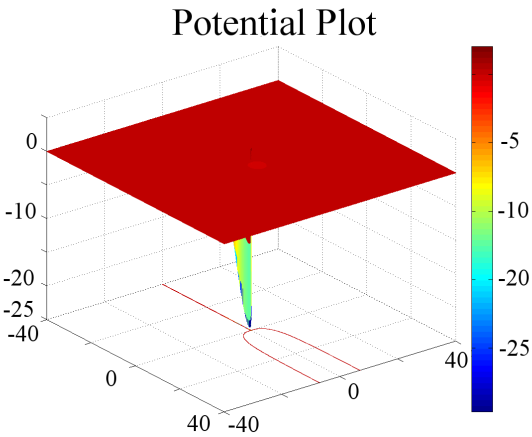


Figure 7: The effective potential energy of Eq.(19) corresponding to the displacement function of Eq.(17). In this figure, $b = 1$ and $k = 10$.

¹ O. Penrose and L. Onsager, Phys. Rev. **104**, 576 (1956); G. V. Chester and L. Reatto, Phys. Rev. **155**, 88 (1967); A. F. Andreev and I. M. Lifshitz, Sov. Phys. JETP **29**, 1107 (1969); L. Reatto, Phys. Rev. **183**, 334 (1969); A. J. Leggett, Phys. Rev. Lett. **25**, 2543 (1970); P.W. Anderson, Basic Notions of Condensed Matter Physics, (Benjamin, Menlo Park, CA), Ch. 4, 143 (1984); G. G. Batrouni, R.

T. Scalettar, G. T. Zimanyi, and A. P. Kampf, Phys. Rev. Lett. **74**, 2527 (1995); G. G. Batrouni and R. T. Scalettar, Computer Physics Communications **97**, 63 (1996); D. M. Ceperley and B. Bernu, Phys. Rev. Lett. **93**, 155303 (2004); W. Saslow, Phys. Rev. B **71**, 092502 (2005); T. Suzuki and N. Kawashima, Phys. Rev. B **75**, 180502 (R) (2007); A. Stoffel and M. Gulacsi, Europhysics Letters **85**,

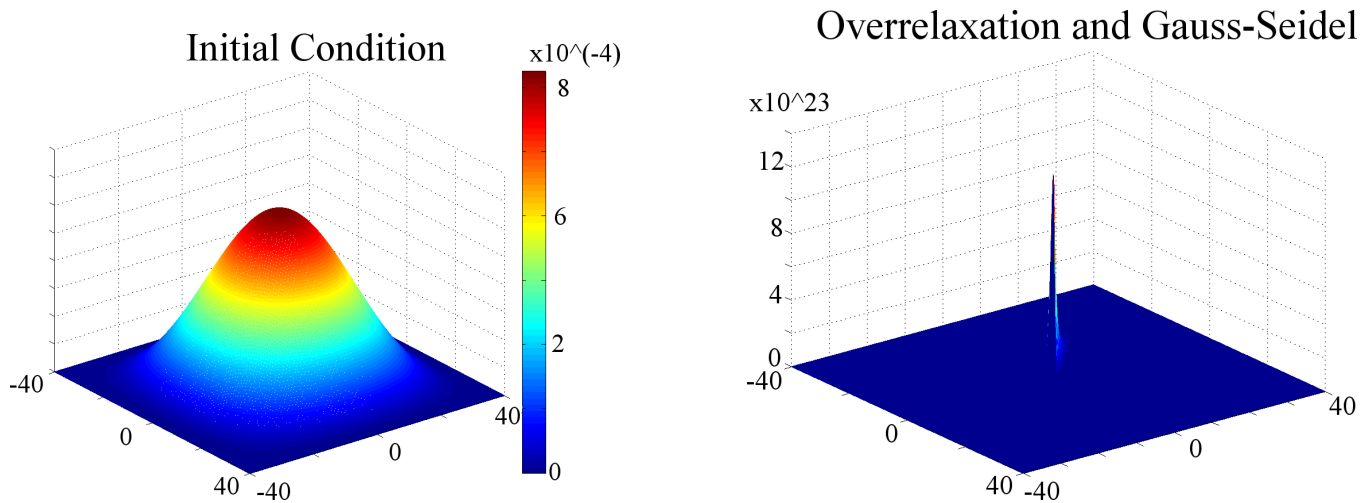


Figure 8: The supersolid order parameter associated with the effective potential of Fig.(7). Shown is the Gauss-Seidel solution of Eqs.(3, 4) with $c = 1$ for the dislocation profile of Eq.(17). Left: An initial seed state. Right: The final “wavefunction” (supersolid order parameter). The localized bound state is evident

- 20009 (2009).
- ² G.V. Chester, Phys. Rev. A **2**, 256 (1970).
- ³ N. Prokof'ev, Adv. in Phys. **56** 2, 381 (2007).
- ⁴ E. Kim and M. H. Chan, Science **305**, 1941 (2004); E. Kim, M. H. W. Chan, Nature **427**, 225 (2004); J. Beamish, Nature **427**, 204 (2004).
- ⁵ S. Sasaki, R. Ishiguro, F. Caupin, H. J. Maris, and S. Balibar, Science **313**, 1098 (2006).
- ⁶ P. Phillips and A. Balatsky, Science, **316**, 1435 (2007).
- ⁷ F. London, *Superfluids* (Wiley, New York (1954)), vol. II, p. 144.
- ⁸ G. B. Hess and W. M. Fairbank, Phys. Rev. Lett. **19**, 216 (1967).
- ⁹ E. I. Andronikashvili, J. Phys. (USSR) **10**, 201 (1946); E. I. Andronikashvili and Yu. G. Mamaladze, Rev. Mod. Phys. **38**, 567 (1966).
- ¹⁰ A. V. Balatsky, Z. Nussinov, M. J. Graf, S. A. Trugman, Phys. Rev. B **75**, 094201 (2007); Z. Nussinov, A. V. Balatsky, M. J. Graf, and S. A. Trugman, Phys. Rev. B **76**, 014530 (2007); M.J. Graf, A.V. Balatsky, Z. Nussinov, I. Grigorenko, and S.A. Trugman, J. Phys.: Conf. Ser. **150**, 032025 (2009); M. J. Graf, Z. Nussinov, and A. V. Balatsky, arXiv:0907.4965
- ¹¹ A. S. C. Rittner and J. D. Reppy, Phys. Rev. Lett. **98**, 175302 (2007).
- ¹² Y. Aoki, M. C. Keiderling, and H. Kojima, Phys. Rev. Lett. **100**, 215303 (2008).
- ¹³ C-D. Yoo and A. Dorsey, Phys. Rev. B **79**, 100504 (2009).
- ¹⁴ D. A. Huse and Z. U. Khandker, Phys. Rev. B **75**, 212504 (2007).
- ¹⁵ M. Boninsegni, N. Prokofev, and B. Svistunov, Phys. Rev. Lett. **96**, 105301 (2006); J. Wu and P. Phillips, Phys. Rev. B **78**, 014515 (2008); G. Biroli, C. Chamon, and F. Zamponi, Phys. Rev. B **78**, 224306 (2008); Z. Nussinov, Physics **1**, 40 (2008).
- ¹⁶ J. Zannen, Z. Nussinov, and S. I. Mukhin, Ann. Phys. **310**, 181 (2004); V. Cvetkovic and J. Zaanen, Phys. Rev. Lett. **97**, 045701 (2006); V. Cvetkovic, Z. Nussinov, S. Mukhin, and J. Zaanen, Europhys. Lett. **81**, 27001 (2008).
- ¹⁷ A. V. Balatsky and E. Abrahams, J. of Superconductivity and Novel Magnetism **19**, 395 (2006).
- ¹⁸ A. T. Dorsey, P. M. Goldbart, and J. Toner, Phys. Rev. Lett. **96**, 055301 (2006).
- ¹⁹ J. Toner, Phys. Rev. Lett. **100**, 035302 (2008)
- ²⁰ J. Day and J. Beamish, Phys. Rev. Lett. **96**, 105304 (2006); *ibid.* Nature (London) **450**, 853 (2007).
- ²¹ A. Koga, T. Higashiyama, K. Inaba, S. Suga, and N. Kawakami, J. Phys. Soc. Japan **77**, 073602 (2008).
- ²² P. Sengupta and C. D. Batista, Phys. Rev. Lett. **98**, 227201 (2007).
- ²³ For a review, see Lattice Effects in High- T_c Superconductors, eds. Y. Bar-yam, T. Egami, J. Mustre-de Leon, and A. R. Bishop (World Scientific, Singapore, 1992); Nanoscale Phase Separation and Colossal Magnetoresistance, ed. E. Dagotto (Springer, New York, 2003); Intrinsic Multiscale Structure and Dynamics in Complex Electronic Oxides, eds. A. R. Bishop, S. R. Shenoy, and S. Sridhar (World Scientific, Singapore, 2003).
- ²⁴ Jian-Xin Zhu, K. H. Ahn, Z. Nussinov, T. Lookman, A. V. Balatsky, and A. R. Bishop, Phys. Rev. Lett. **91**, 057004 (2003).
- ²⁵ L. D. Landau and E. M. Lifshitz, *Statistical Physics Part 2*, Butterworth-Heinemann, Boston (1999).
- ²⁶ M. Tinkham, *Introduction to Superconductivity*, 2nd edition, McGraw-Hill, New York (1996).
- ²⁷ J. Friedel, *Dislocations*, Pergamon press, New York, 1954; F. R. N. Nabarro, *Theory of Dislocations*, Clarendon, Oxford, 1967; J. P. Hirth and J. Lothe, *Theory of Dislocations*, McGraw- Hill, New York, 1968; H. Kleinert, *Gauge fields in Condensed Matter*, Vol. II: Stresses and Defects, Differential Geometry, Crystal Defects (World Scientific, Singapore, 1989).
- ²⁸ J. A. Aronovitz, P. Goldbart, and G. Mouzurkewich, Phys. Rev. Lett. **64**, 2799 (1990).
- ²⁹ Eq.(3) could also be solved in the presence of the cubic term, albeit not giving any new insight relative to our linearized differential equation of Eq.(4). Throughout this work, we will assume a system that is symmetric about the origin, with a unidirectional axis of length L along which the displacements occur ($-L/2 \leq z \leq L/2$). For real ψ ,

with boundary condition $\psi(z = -L/2) = 0$, multiplying Eq.(3) by ψ and integrating, we arrive at the general implicit relation

$$z(\psi) = -\frac{L}{2} + \int_0^\psi \frac{d\tilde{\psi}}{\tilde{\psi}} \sqrt{-\frac{c}{a + b\tilde{\psi}^2 + \lambda(z)}}, \quad (24)$$

for $z < 0$. For $z > 0$, for a system with displacements that are symmetric about $z = 0$, $\psi(z) = \psi(-z)$.